Flood inundations and risk mapping in a tidal river: a case study for the Kelani River basin, Sri Lanka

Jayanaga Thanuka Samarasinghe
Sri Lanka Technological Campus
Eranda Perera
Sri Lanka Technological Campus
Fang Yenn Teo
University of Nottingham Malaysia Faculty of Engineering
Andy Chan
University of Nottingham Malaysia Faculty of Engineering
Surajit Ghosh (S.GHOSH@CGIAR.ORG)
International Water Management Institute https://orcid.org/0000-0002-3928-2135

Research Article

Keywords:

Posted Date: June 22nd, 2021

DOI: https://doi.org/10.21203/rs.3.rs-161788/v1

Flood inundations and risk mapping in a tidal river: a case study for the Kelani River basin, Sri Lanka

Jayanaga Thanuka Samarasinghe[1], Eranda Perera[*2], Fang Yenn Teo[3], Andy Chan[4], Surajit Ghosh[5]

[1]Research Assistant, Department of Civil Engineering, Sri Lanka Technological Campus, Padukka, Sri Lanka. Email: jsamarasi94@gmail.com

[2]Senior Lecturer, Department of Civil Engineering, Sri Lanka Technological Campus, Padukka, Sri Lanka (corresponding author). ORCID: https://orcid.org/0000-0001-7885-7651. Email: dferanda.perera@gmail.com

[3]Associate Professor, Department of Civil Engineering, University of Nottingham Malaysia, Semenyih, Malaysia. ORCID: https://orcid.org/0000-0002-5529-1381. Email: fangyenn.teo@nottingham.edu.my

[4]Professor, Department of Civil Engineering, University of Nottingham Malaysia, Semenyih, Malaysia. ORCID: https://orcid.org/0000-0003-2267-4949. Email: andy.chan@nottingham.edu.my

[5]Regional Researcher, International Water Management Institute, Colombo, Sri Lanka. ORCID: https://orcid.org/0000-0002-3928-2135. Email: s.ghosh@cgiar.org

Flood inundations and risk mapping in a tidal river: a case study for the Kelani River basin, Sri Lanka

Abstract

The downstream low-lying regions of the Kelani River, including some areas in the Districts of Colombo and Gampaha, Sri Lanka, frequently face severe inundations due to extreme rainfalls in the upper basin. In the present study, 1-D and 2-D hydrodynamic models in HEC-RAS have been used to examine the flood inundations in the tidal influenced Kelani River with ground observations and remote sensing. The HEC-RAS model has been used to produce a flood hazard map for hazard assessment in the lower Kelani River basin under different return periods. Furthermore, expected discharges for different return periods have been estimated using the hydrological model HEC–HMS with the updated intensity depth frequency curves for the Kelani River basin. Sentinel 1 imagery and field survey results are used to validate the simulated flood inundation extent; hydrodynamic model results validated against observed stage measurements; hydrological model validated against discharge measurements. Further, the validated hydrodynamic model showed the high capability to capture flow processes (Nash-Sutcliffe coefficient = 0.90 and Pearson coefficient of correlation = 0.95) along with inundation extent (Success Index = 0.90) of selected historical extreme events. Then the hydrological model is used to predict the flows of the Kelani River basin with a good agreement (Nash-Sutcliffe coefficient = 0.91 and the Pearson coefficient of correlation = 0.93). Finally, flood risk zoning for different return periods are developed based on the present model which would be a useful benchmark to design and implement flood control and mitigation measures for the river basin.

Keywords Kelani River, Flood inundation modelling, Flood hazard mapping, Flood Risk analysis.

1 Introduction

Each year millions of families from different parts of the world are affected due to floods, causing US$662 billion in damages since 1995 (UNISDR 2015). In South Asian, most townships and urban cities are located at popular flood risk areas (Tariq 2011). Urbanisation and associated fast growing of people living in cities of South Asian have led to an increase of unplanned and uncontrolled land development activities (Shah et al. 2020). These activities particularly involved floodplains in the cities can potentially increase the flood hazard risks (Baker 2012; Teo et al. 2012a, b; Egbinola et al. 2017 to mention but a few), particularly for most of the cities in South Asian (Pervin et al. 2020). These adverse risks and impacts of flood range from direct impacts such as loss of human life, damages to property, destruction of crops, loss of livestock to indirect impacts such as the spread of waterborne diseases, deterioration of drinking water quality, etc. Therefore, the ability to predict the nature and the extent of the flood is very important to the local decision-makers as this would enable them to plan for such adverse impacts and minimize the damage.

It is essential to develop appropriate mitigation measures to minimize flood risk and damage. There are mainly two flood mitigation approaches: structural and non-structural. A few structural measures are dykes, dams, flood control reservoirs, diversions, flood-ways, etc. On the other hand, flood forecasting and warning, watershed management, floodplain development guidelines, insurance, and awareness programmes fall into non-structural measures (Nandalal 2009; Caddis et al. 2012; to mention but a few). The structural measures have a certain design capacity, and in case of flood levels exceed, there is a possibility of failure and the damage could be disastrous. Therefore, non-structural approaches are very important to promote settlement, reduce property damages ensuring safety, and well-being of the public.

The use of hydrodynamic simulation to forecast flood extent in the Kelani River is particularly important for water managers and decision-makers in Sri Lanka. The river basin has significant socio-economic benefit. The commercial and administrative capital of Sri Lanka is located in the lower basin of Kelani River. The District of Colombo, with a population of 2.2

74 million, is concentrated within an area of 642 km^2, has a population density approximately 10
75 times the remaining parts of the island (i.e. estimated with mid-year population 2013-2018
76 census and statistics). The urbanization also affects the rainfall-runoff and drainage
77 mechanisms in the lower basin of the river. In the past few decades, floods frequently occurred
78 and caused significant economic losses to the country and disruptions to the lives of
79 communities living along and around riverbanks (CRIP 2018). Additionally, Kelani River plays
80 a crucial role in power generation and in providing water supply facility to millions of people in
81 Sri Lanka (Sivapalasundaram et al. 2015).

82 The work in this study is built on the work of De Silva et al. 2012 who used a grid-based
83 Flo-2D model to simulate floods in the Kelani River, whereas the present work employs a
84 mesh-based HEC-RAS (Hydraulic Engineering Center River Analysis System) model. To
85 improve the accuracy of the model, the authors take into consideration the tidal influence on
86 the river flood, which Gunathilaka et al. 2010 and JAICA (2009) have also shown to be of
87 significance especially near to the Nagalagam station, which is closed to river mouth. Further,
88 a higher accuracy DEM (i.e. 4m resolution) used here in comparison to 10m resolution of De
89 Silva et al. (2012)'s model. Additionally, the model calibration conducted by De Silva et al.
90 (2012) follows a statistical approach using rainfall and discharge data, whereas we use field
91 observations to calibrate the model. With an improved modelling approach, more accurate
92 DEM and field observations for model calibration, the present work presents more accurate
93 simulation results for flood inundation extent, water depth and discharge for selected floods in
94 the last couple of decades. Then the results have been validated against both satellite images
95 as well as field measurements providing higher confidence of the model performance.

96 After the model validation, it is used to simulate 10, 25, 50 and 100 year return period
97 floods in the river basin and to produce flood risk map based on analysis of building and
98 population. For future use, design charts have been prepared based on the model results and
99 impact due to floods to different regions in the river basin. This paper is organized as follows.
100 Firstly, the study area and collected data for the study are presented. Then the model used is
101 briefly introduced. Next, an overview of the methodology provided with various statistical

techniques used to quantify and assess the performance of the present model. Then the present model's validation is presented, along with model results for flood inundation extents for various return periods. Additionally, building and population related flood risk maps are also presented. Finally, conclusions are presented in the last section.

2 Study Area and Data

2.1 Study Area

The Kelani River originates from the central hills and flows West coast through Colombo city. The basin is located between Northern latitude 6° 47' to 7° 05' and Eastern longitudes 79° 52' to 80° 13', with a river basin area of nearly 2,230 km^2 as shown in Fig. 1. Broadly, the river basin can be categorized into upper and lower basins. The upper basin features mountainous terrain, whereas the lower basin is generally flat terrain. The lower basin lies below the Hanwella River gauging station which has an approximate area of 500 km^2.

The upper basin is covered predominantly with vegetation, whereas the lower basin is heavily urbanized. The river basin receives an average annual rainfall of nearly 2,400 mm and carries a peak discharge of 800 − 1,500 m^3/s during the monsoonal periods (i.e. especially in South-West monsoon period from May to September). Frequently, during the South-West monsoon period, the lower reach of the basin is subjected to flooding as recorded from the flood gauge located at Nagalagam Street.

2.2 Data

The data collected for the present project included precipitation data, stream flow data, land-use characteristics data, flood field measurements, satellite images and a Digital Elevation Model (DEM) of the river basin. Table 1 summarizes the data and their resolutions collected from different sources.

3 Methodology

The present work employs a coupled hydrodynamic and hydrological model with information being fed between the models according to the flow chart shown in Fig. 2. In addition to the

inputs to the model, the figure also shows the validation checks conducted on the output. After the validation, the HEC-HMS provides the input flow for return period floods in the HEC-RAS model. Then the HEC-RAS is used to produce hazard maps and risk analysis due to the floods.

3.1 Hydrodynamic Model

In the present study, the public domain software HEC-RAS is used to simulate the flood inundation extent with unsteady flows. For higher accuracy, the integrated approach of combined 1D and 2D as suggested by Horritt and Bates (2002), Werner (2004), Betsholtz and Nordlöf (2017), Das et al. (2018), and Lea et al. (2019) are employed in the present model. Furthermore, to capture tidal behaviour, the full momentum equation is applied following the approach of Brunner (2016a). Subsequently, a terrain modification is conducted to complement the river bathymetry with measured cross-sections; river discharge and tides are maintained as the upper and lower boundary conditions respectively.

The Kelani River is a tidal influenced river Hettiarachchi (2020) and Gunathilaka et al. (2010) as demonstrated by the gauge readings at Nagalagam Street. Therefore, the downstream boundary conditions are set to be the measured tidal data for all the cases. These effects are incorporated to the present model following the approach of by Brunner (2016b), JAICA (2009), and Bakhtyar et al. (2020).

3.2 Hydrological Model

The public domain software Hydraulic Engineering Center Hydraulic Modelling System (HEC-HMS) is used to simulate precipitation runoff process in this study using an event-based approach. Following the work of De Silva et al. (2014), the Green and Ampt model, the Clark Unit hydrograph and the recession method are employed in the present study (Scharffenberg and Fleming 2006).

3.3 Model calibration

3.3.1 Calibration of Hydrodynamic Model

The calibration of the hydrodynamic model was conducted using the May-2018 flood event (low return period discharge). The calibration was conducted by fine-tuning the Manning's roughness coefficients for stream and flood plains (Chow 1959). Observed water depth,

158 inundation extent and recorded high flood levels (HFL) are used to calibrate the hydrodynamic
159 model. Further, cross-section spacing, time-step and optimum mesh size selected for the
160 model following the suggestions in Samuels (1989), Brunner (2016b) and Betsholtz and
161 Nordlöf (2017).

162 Additionally, the present modelling approach takes into account the tidal effects at the
163 sea outfall where the sea outfall is set as one of the boundaries with the stage computed using
164 Admiralty tide tables (UKHO 2004) and an external model following the approach of JAICA
165 (2009) and Bakhtyar et al. (2020). As Kelani River is a tidally influenced river, Gunathilaka et
166 al. (2010) showed that the high tide during flood events would create the worst-case scenario
167 in the vicinity of Nagalagam Street. Further, for the purpose of mapping inundation return
168 periods in the HEC-HMS model, a uniform 1m stage is set as the lower boundary condition.
169 Subsequently, the sea level rise and the Coriolis effects are not incorporated in the present
170 study due to its low significance in floods.

171 The evaluation of performances of model stage and the observed stage is statically
172 evaluated with Nash- Sutcliffe Efficiency Coefficient (NSE) and the Pearson coefficient of
173 determination (R^2). In addition, to evaluate the performances of inundation prediction we
174 followed previous studies (De Silva et al. 2012; Khaing et al. 2019) to conduct a
175 comprehensive evaluation by comparing the satellite observations and model predictions on
176 a cell-by-cell basis following statistical matrix by Falter et al. (2013), Bennett et al. (2013),
177 Falter et al. (2015) and Khaing et al. (2019).

178 (a) Flood Area Index (FAI)

179 $$FAI = \frac{M_1 D_1}{M_1 D_1 + M_1 D_0 + M_0 D_1} \quad (1)$$

180 (b) Accuracy

181 $$Accuracy = \frac{hits + correct\ negatives}{total} \quad (2)$$

182 (c) Bias Score

183 $$Bias\ score = \frac{hits + flase\ alarms}{hits + misses} \quad (3)$$

184 (d) Probability of detection (hit rate)

$$Probability\ of\ detection\ (hit\ rate) = \frac{hits}{hits+misses} \quad (4)$$

(e) False alarm ratio

$$False\ alarm\ ratio = \frac{flase\ alarms}{hits+flase\ alarms} \quad (5)$$

(f) Probability of false detection

$$Probability\ of\ false\ detection\ (flase\ alarm\ rate) = \frac{false\ alarms}{correct\ negatives+flase\ alarms} \quad (6)$$

(g) Success index

$$Sucess\ index = \frac{1}{2}\left(\frac{hits}{hits+misses} + \frac{correct\ negatives}{correct\ negatives+flase\ alarms}\right) \quad (7)$$

where, M_1D_1 number of grid cells is correctly predicted as flooded by model (hits), M_1D_0 is number of cells flooded in the prediction but observed as dry in the observation (false alarm), M_0D_1 is the predicted dry area but observed wet area (misses), and number of correct negatives are the cells predicted and observed as dry.

3.3.2 Calibration of Hydrological Model

May-2017 flood event was used for the hydrological model calibration by adjusting soil and base flow parameters until the goodness of fit achieved to be in the acceptable range of Moriasi et al. (2007). To evaluate the model performance statistically, a skill matrix was used.

Further, updated Intensity Depth Frequency (IDF) curves used for the model development which takes into account climate change effects as well (Nandalal and Ghnanapala 2017) with 3-day rainfall.

(a) Pearson coefficient of determination (R^2):

$$R^2 = \frac{\left[\sum_{i=1}^{n}((O_i-\bar{O})\times(S_i-\bar{S}))\right]^2}{\sum_{i=1}^{n}(O_i-\bar{O})^2\times\sum_{i=1}^{n}(S_i-\bar{S})^2} \quad (8)$$

(b) Nash Sutcliffe Efficiency Coefficient (NSE):

$$NSE = 1 - \frac{\Sigma_{i=1}^{n}(S_i-O_i)^2}{\Sigma_{i=1}^{n}(O_i-\bar{O})^2} \quad (9)$$

(c) Percentage of Bias (PBIAS):

$$PBIAS = \left|\frac{\sum_{i=1}^{n}(S_i - O_i)}{\sum_{i=1}^{n} O_i}\right| \times 100\% \quad (10)$$

(d) Root Mean Square Error (RMSE):

$$RSR = \frac{[\sqrt{\sum_{i=1}^{n}(O_i - S_i)^2}]}{\sqrt{\sum_{i=1}^{n}(O_i - \bar{S}_i)^2}} \quad (11)$$

where O_i is observed flow at i[th] time, S_i is simulated flow at i[th] time, $\bar{O}$ is mean of observed flow and $\bar{S}$ is mean of simulated flow respectively.

3.4 Satellite Image Processing and Flood Hazard Mapping

The open-access micro wave satellite images from Sentinel – 1 during flood events were processed with the method suggested by Perrou et al. (2018) with the use of open-source software SNAP v8.0 (http://step.esa.int/main/toolboxes/snap/). The reason for the selection of Sentinel-1 compared to other satellite missions were described by Psomiadis (2016), Khaing et al. (2019), Bioresita et al. (2018) and DeVries et al. (2020).

For the present study, hazard induced by water depth is considered due to the scarcity of data related to the velocities, the inundation time or the time to the rise of flood wave. A lower hazard rank is assigned to a lower water depth while a larger hazard rank is employed to indicate a higher hazard (De Silva et al. 2012). Table 2 shows the rank and hazard levels employed in the present study relative to the Nagalagam Street gauge reading (0 MSL).

3.5 Flood Vulnerability

The vulnerability was classified into population and building vulnerability. Both population and building vulnerabilities were analyzed based on the age groups and building materials respectively in each GN (*Grama Niladari*) division. In the present study, the population's vulnerability to flood was computed using population data obtained from the 2012 census.

In population vulnerability, the highest ranks are assigned to age groups less than 5 years and above 60 years as they are deemed to be more vulnerable. Low and intermediate ranks are assigned to the age group of 26 to 59 year and 6 to 25 years respectively. At the

same time, to assess building vulnerability, the highest ranks are given to buildings that are susceptible to damage due to minimal impact.

The vulnerability index for each categorization in GN division was calculated by following Samarasinghe et al. (2010):

$$VI_{GN} = \sum_{i=1}^{n} F\ GN_i \times R_i \quad (12)$$

where: VI_{GN} is vulnerability in a GN division (-), $F\ GN_i$ is a fraction of age group/building material type out of the total in the GN division, R_i is vulnerability rank of each group (-) and n is number of categories respectively.

The vulnerability index calculated using equation (12) was standardized by overlaying with the present model's inundation extents to obtain revised vulnerability index for various return periods in the Kelani River basin (as shown in Table 3):

3.6 Flood Risk

The risk maps for various return period floods are computed by assuming the equation suggested by Wolfgang (2005) and Samarasinghe et al. (2010), i.e. $Risk\ index = Hazard\ index \times Vulnerability\ index$. The Table 4 shows the risk classification employed in the present study.

4 Results and discussion

4.1 Hydrodynamic model validation

The stages simulated by the model at the Stations of Hanwella and Nagalagam Street are compared with the measured stage values of those stations (Table 5). The comparison shows close agreement between the results as indicated by high R^2 and NSE values (i.e. $R^2 = 0.93$, NSE = 0.92 at Hanwella Gauge and $R^2 = 0.95$, NSE = 0.94 at Nagalagam Street gauge). The results showed that the HEC-RAS hydrodynamic model is able to capture the temporal variability of the flood flow process very well. However, the comparisons also revealed that the model underestimates the stage on many occasions (Fig. 3). It is understood that the

cause for this underestimation is primarily resulting from the negligence of rainfall-runoff at the lower basin in the model.

The simulated flood inundations for the 2018 and 2016 events are compared against field survey measurements and satellite images in Figs. 4 and 5. For a clear comparison between different regions of the Kelani River basin, the area is subdivided into 10 regions and each of the regions compared between simulated and survey measurements/ satellite images, as shown in Table 6.

Model simulated inundation comparison with satellite observed inundation related to May-2018 showed that there is an 83% of hit rate and 94 % of accuracy. This shows that the model was able to realistically capture the inundation process. But, at the same time 34% of false alarm ratio, 5% of false alarm rate and 1.35 bias score depicted that model tends to overestimate. Additionally, the May-2018 event simulation was able to correctly capture the flood extent with 88% of success index. Further, the May-2016 event simulation was able to detect the observed flood with 97% hit rate and an accuracy of 87%. Although the false alarm rate and the false alarm ratios increased to 48% and 13% respectively, the results show that the model tends to overestimate the inundations with 1.9 bias score. This also indicated the model could successfully detect inundations (i.e. success index) with 91%. On average the model results showed that there is a high hit rate of 90% and accuracy of 91%, although the results displayed relatively small overestimation in 41% of false alarm ratio, 9% of false alarm rate together with 1.65 bias score. This validation of the model showed it is able to successfully detect the flood with 90% of the success index.

Further, average comparison of simulated flood during the surveyed inundation period, in both events shows that there is a high accuracy (i.e. 90%) but the hit rate was 61% as well as the false alarm rate and the ratios were 17% and 3% with 0.815 bias score. This suggests that the model underestimates the inundations relative to the surveyed inundations. All together 78% success index was obtained. Compared to satellite observed inundations, the comparison of surveyed inundation is not very accurate and also it is observed that surveyed inundations underestimate satellite observations as shown by Figs. 4 and 5.

After the present model validation provided sufficient confidence in its capabilities, it is then used for estimating the risk for population and building under various return periods

4.2 Hydrological model validation

Fig.6 shows the comparison between the present model's simulated and the observed discharge for 2017, 2011 and 2010 flood events. The simulated results agree closely with the observed flows, as evidenced by the goodness of fit tests given in Table 7. The results supported the recommendation of De Silva et al. (2014) that the Green and Ampt model is ideal for the Kelani River basin. However, the loss parameters slightly deviated from the corresponding values of De Silva et al. (2014), which may have resulted in a slight over prediction.

Table 8 shows the 3-day total rainfall and the expected discharges derived from the HEC-HMS model using IDF curves. Based on these results, the Kelani River basin appears to have faced only a maximum flood of 10-year return period; Table 8 is a good assessment of potential damage for higher return periods.

4.3 Hazard Mapping and Risk Zoning

Flood hazard mapping for different return periods were conducted with estimated discharges from the previously validated models. According to Tables 9, 15 out of 26 divisional secretariat (DS) divisions of both Colombo and Gampaha districts are identified as hazardous. Under different return periods, the magnitude and scale of flooding varied for different regions as summarized in Supplementary Table 1. Further, the water depths are classified into 5 groups based on the Nagalagam Street warning levels (i.e. 0.2m – 1.5m, 1.5m – 2.13m, 2.13m – 2.70m, 2.70m-3.65m and above 3.65m). Based on the results mentioned in Supplementary Table 1, a total area of 68.06, 95.56, 99.51 and 101.69 square kilometres of lower Kelani River basin subjected to flood under 10year, 25year, 50year and 100 year return periods respectively.

During this study we considered vulnerability in terms of population and buildings. Fig. 8 shows the variation of population risk under different return period floods. The results extracted from the maps mentioned in Supplementary Table 2 summarizes the results. Fig. 7

318 (a) shows Kaduwela, Seethawaka, Kolonnawa, Dompe and Biyagama DS divisions are under
319 higher risk than the other DS divisions as a result of low-lying land with high population density.
320 The evaluation of risk in terms of buildings shows similar behaviour to that with the
321 population (see Fig. 9) but there is an increase in the building risk areas (Fig. 7 and Tables 9
322 and 11). Kaduwela, Homagama, Seethawaka, Dompe, Biyagama, and Kolonnawa DS
323 divisions are sub-urban areas with the concentrated population as well as semi-permanent
324 structures which can susceptible to any damage at any moment (based on census data).
325 Additionally, most of the industrial zones of Sri Lanka concentrated and established at both
326 banks of the Kelani River. From the risk analysis, it is shown that both population and buildings
327 in Biyagama, Dompe, Seethawaka, Homagama and Kolonnawa DS divisions can be identified
328 as high-risk zones.
329
330 **5 Conclusions**
331 HEC-RAS coupled model can realistically estimate the inundation extents during a flood in a
332 tidal influenced river. This study showed that the numerical models well captured the
333 inundation observed from the satellite images than the surveyed inundations. Further, a well-
334 validated model can be used to estimate the inundations that can be caused as a result of
335 extreme flood events. The corresponding expected discharges for extreme rainfall events can
336 be calculated from the HEC-HMS event based model. Additionally, this study validated the
337 statement of “Green Ampt model successfully predict the flows for Kelani River basin”.
338 The flood in lower Kelani River basin showed that 15 of them out of 26 DS divisions of
339 both Districts of Colombo and Gampaha are under hazard level. But, when assessing the risk
340 in terms of both population and buildings, 13 divisions can be considered as risk zones.
341 Additionally, Kaduwela, Homgama, Biyagama, Dompe, Seethawaka and Kolonnawa can be
342 considered as high-risk zones.
343 These findings are useful for planning and to propose implementation strategies to
344 minimize flood damages in the Lower Kelani River basin. The approaches in this study can
345 help to estimate the flood damage and evacuate the people who are susceptible to more risk.

Also, the approached can be used as an early warning system anywhere in the world with people live in floodplain along river.

Acknowledgement

The authors would like to acknowledge the Climate Resilience Improvement Project (CRIP), Ministry of Irrigation and Water Resources Management Sri Lanka, the Survey Department of Sri Lanka, the Meteorological Department of Sri Lanka and the Irrigation Department of Sri Lanka for sharing data for this project. Further, the authors would also like to acknowledge the Disaster Management Center of Sri Lanka and the Department of Census and Statistics of Sri Lanka for sharing information for this project.

Declarations

Funding

This work is funded by the Responsive Research Seed Grant of Sri Lanka Technological Campus, Padukka, Sri Lanka under grant no. RRSG/20/A6.

Conflicts of interest/Competing interests

The authors declare that they have no conflict of interest.

Availability of data and material

The data and material that support the findings of this study are available from the corresponding author, upon reasonable request.

Code availability

The primary software used to generate the simulation results, HEC-RAS and HEC-HMS, are freely accessible open-source software.

Authors' contributions

E.P and J.T.S conceived of the presented idea. J.T.S developed the model and conducted the simulations. J.T.S validated the model simulations against measured data. E.P encouraged J.T.S to investigate flood vulnerability of the basin and supervised the findings of this work.

S.G improved discussion and analysis and improved the quality of figures. All authors discussed the results and contributed to the final manuscript.

References

Baker JL (2012) Climate change, disaster risk, and the urban poor: cities building resilience for a changing world. The World Bank. https://doi.org/10.1596/978-0-8213-8845-7

Bakhtyar R, Maitaria K, Velissariou P, et al (2020) A new 1D/2D coupled modeling approach for a riverine-estuarine system under storm events: Application to Delaware River Basin. Journal of Geophysical Research: Oceans 125. https://doi.org/10.1029/2019JC015822

Bennett ND, Croke BF, Guariso G, et al (2013) Characterising performance of environmental models. Environmental Modelling & Software 40:1–20. https://doi.org/10.1016/j.envsoft.2012.09.011

Betsholtz A, Nordlöf B (2017) Potentials and limitations of 1D, 2D and coupled 1D-2D flood modelling in HEC-RAS. TVVR17/5003

Bioresita F, Puissant A, Stumpf A, Malet J-P (2018) A method for automatic and rapid mapping of water surfaces from sentinel-1 imagery. Remote Sensing 10:217. https://doi.org/10.3390/rs10020217

Brunner G (2016a) Combined 1D and 2D Modelling with HEC–RAS, v. 5. US Army Corps of Engineers

Brunner G (2016b) HEC-RAS 5.0 2D Modeling User's Manual. Davis, CA

Caddis B, Nielsen C, Hong W, et al (2012) Guidelines for floodplain development–a Malaysian case study. International journal of river basin management 10:161–170. https://doi.org/10.1080/15715124.2012.688750

Chow V (1959) T. 1959 Open-Channel Hydraulics. McGraw Hill

CRIP (2018) Strategic Environmental Assessment of Development of River Basin Level Flood and Drought Mitigation Investment Plans (DBIP). http://crip.lk/wp-content/uploads/2019/01/Kelani-River-SEA-Study-Final-Report.pdf. Accessed 2 May 2020

Das P, Khan AHAN, Islam F, et al (2018) Flood Inundation Mapping on Surma-Kusiyara Floodplain Using HEC-RAS 1D/2D Couple Model

De Silva M, Weerakoon S, Herath S, et al (2012) Flood Inundation Mapping along the Lower Reach of Kelani River Basin under the Impact of Climatic Change. Engineer 45:23–29

De Silva M, Weerakoon S, Herath S (2014) Modeling of event and continuous flow hydrographs with HEC–HMS: case study in the Kelani River Basin, Sri Lanka. Journal of Hydrologic Engineering 19:800–806. https://doi.org/10.1061/(ASCE)HE.1943-5584.0000846

DeVries B, Huang C, Armston J, et al (2020) Rapid and robust monitoring of flood events using Sentinel-1 and Landsat data on the Google Earth Engine. Remote Sensing of Environment 240:111664. https://doi.org/10.1016/j.rse.2020.111664

Egbinola C, Olaniran H, Amanambu A (2017) Flood management in cities of developing countries: the example of Ibadan, Nigeria. Journal of Flood Risk Management 10:546–554. https://doi.org/10.1111/jfr3.12157

Falter D, Schröter K, Dung NV, et al (2015) Spatially coherent flood risk assessment based on long-term continuous simulation with a coupled model chain. Journal of Hydrology 524:182–193. https://doi.org/10.1016/j.jhydrol.2015.02.021

Falter D, Vorogushyn S, Lhomme J, et al (2013) Hydraulic model evaluation for large-scale flood risk assessments. Hydrological Processes 27:1331–1340. https://doi.org/10.1002/hyp.9553

Gunathilaka M, Wikramanayake W, Perera D, Lanka S (2010) Identifying the impact of tidal level variation on river basin flooding. In: Proceedings of the National Conference on Water, Food Security, and Climate Change in Sri Lanka, BMICH, Colombo, June 9-11, 2009. Volume 2. Water quality, environment, and climate change. IWMI, p 119

Hettiarachchi P (2020) Hydrological Report on the Kelani River Flood in May 2016

Horritt M, Bates P (2002) Evaluation of 1D and 2D numerical models for predicting river flood inundation. Journal of hydrology 268:87–99. https://doi.org/10.1016/S0022-1694(02)00121-X

JAICA (2009) Comprehensive Study on Disaster Management in Sri Lanka Final Report (Supporting Report). https://openjicareport.jica.go.jp/pdf/11931953_01.pdf. Accessed 2 May 2020

Khaing ZM, Zhang K, Sawano H, et al (2019) Flood hazard mapping and assessment in data-scarce Nyaungdon area, Myanmar. PloS one 14. https://doi.org/10.1371/journal.pone.0224558

Lea D, Yeonsu K, Hyunuk A (2019) Case study of HEC-RAS 1D–2D coupling simulation: 2002 Baeksan flood event in Korea. Water 11:2048. https://doi.org/10.3390/w11102048

Moriasi DN, Arnold JG, Van Liew MW, et al (2007) Model evaluation guidelines for systematic quantification of accuracy in watershed simulations. Transactions of the ASABE 50:885–900

Nandalal K (2009) Use of a hydrodynamic model to forecast floods of Kalu River in Sri Lanka. Journal of Flood Risk Management 2:151–158. https://doi.org/10.1111/j.1753-318X.2009.01032.x

Nandalal K, Ghnanapala P (2017) Development of IDF Curves for Colombo. Engineer: Journal of the Institution of Engineers, Sri Lanka 50:

Perrou T, Garioud A, Parcharidis I (2018) Use of Sentinel-1 imagery for flood management in a reservoir-regulated river basin. Frontiers of Earth Science 12:506–520. https://doi.org/10.1007/s11707-018-0711-2

Pervin IA, Rahman SMM, Nepal M, et al (2020) Adapting to urban flooding: a case of two cities in South Asia. Water Policy 22:162–188. https://doi.org/10.2166/wp.2019.174

451 Psomiadis E (2016) Flash flood area mapping utilising SENTINEL-1 radar data. In: Earth
452 Resources and Environmental Remote Sensing/GIS Applications VII. International
453 Society for Optics and Photonics. https://doi.org/10.1117/12.2241055

454 Samarasinghe S, Nandalal H, Weliwitiya D, et al (2010) Application of remote sensing and
455 GIS for flood risk analysis: a case study at Kalu-Ganga River, Sri Lanka. International
456 Archives of the Photogrammetry, Remote Sensing and Spatial Information Science
457 38:110–115.

458 Samuels P (1989) Backwater lengths in rivers. Proceedings of the Institution of Civil Engineers
459 87:571–582. https://doi.org/10.1680/iicep.1989.3779

460 Scharffenberg WA, Fleming MJ (2006) Hydrologic modeling system HEC-HMS: user's
461 manual. US Army Corps of Engineers, Hydrologic Engineering Center

462 Shah SMH, Mustaffa Z, Teo FY, et al (2020) A Review of the Flood Hazard and Risk
463 Management in the South Asian Region, Particularly Pakistan. Scientific African.
464 https://doi.org/10.1016/j.sciaf.2020.e00651

465 Sivapalasundaram, Hettiarachchi P, Piyasena KKA, et al (2015) Hydrological Annual 2014/15.
466 https://www.irrigation.gov.lk/images/pdf/downloads/hydrological%20ann%2014-
467 15.pdf. Accessed 20 May 2020

468 Tariq MAUR (2011) Risk-based planning and optimization of flood management measures in
469 developing countries: Case Pakistan

470 Teo FY, Falconer RA, Lin B, Xia J (2012a) Investigations of hazard risks relating to vehicles
471 moving in flood. The Journal of Water Resources Management 1:52–66

472 Teo FY, Xia J, Falconer RA, Lin B (2012b) Experimental studies on the interaction between
473 vehicles and floodplain flows. International journal of river basin management 10:149–
474 160. https://doi.org/10.1080/15715124.2012.674040

475 UKHO (2004) Admiralty Tide Tables Vol.3: Indian Ocean & South China Sea. United Kingdom
476 Hydrographic Office

477 UNISDR (2015) The human costs of weather related disasters.
478 https://www.unisdr.org/2015/docs/climatechange/COP21_WeatherDisastersReport_2
479 015_FINAL.pdf. Accessed 30 Jun 2020

480 Werner M (2004) A comparison of flood extent modelling approaches through constraining
481 uncertainties on gauge data

482 Wolfgang K (2005) Flood Risk= Hazard. Values. Vulnerability. Water International 30:58–68.
483 https://doi.org/10.1080/02508060508691837

Figures

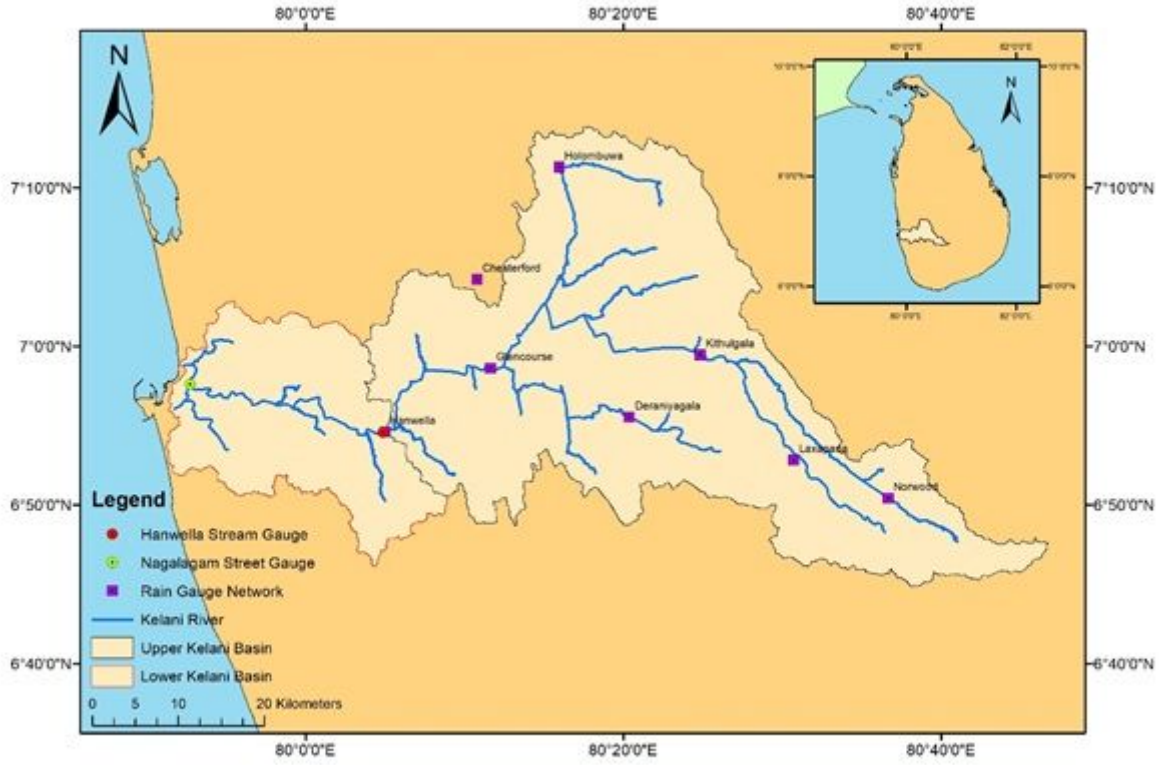

Figure 1

Kelani River basin. The red colour circle shows the Hanwella stream gauge station and the green coloured circle shows stream gauge of Nagalagam Street.

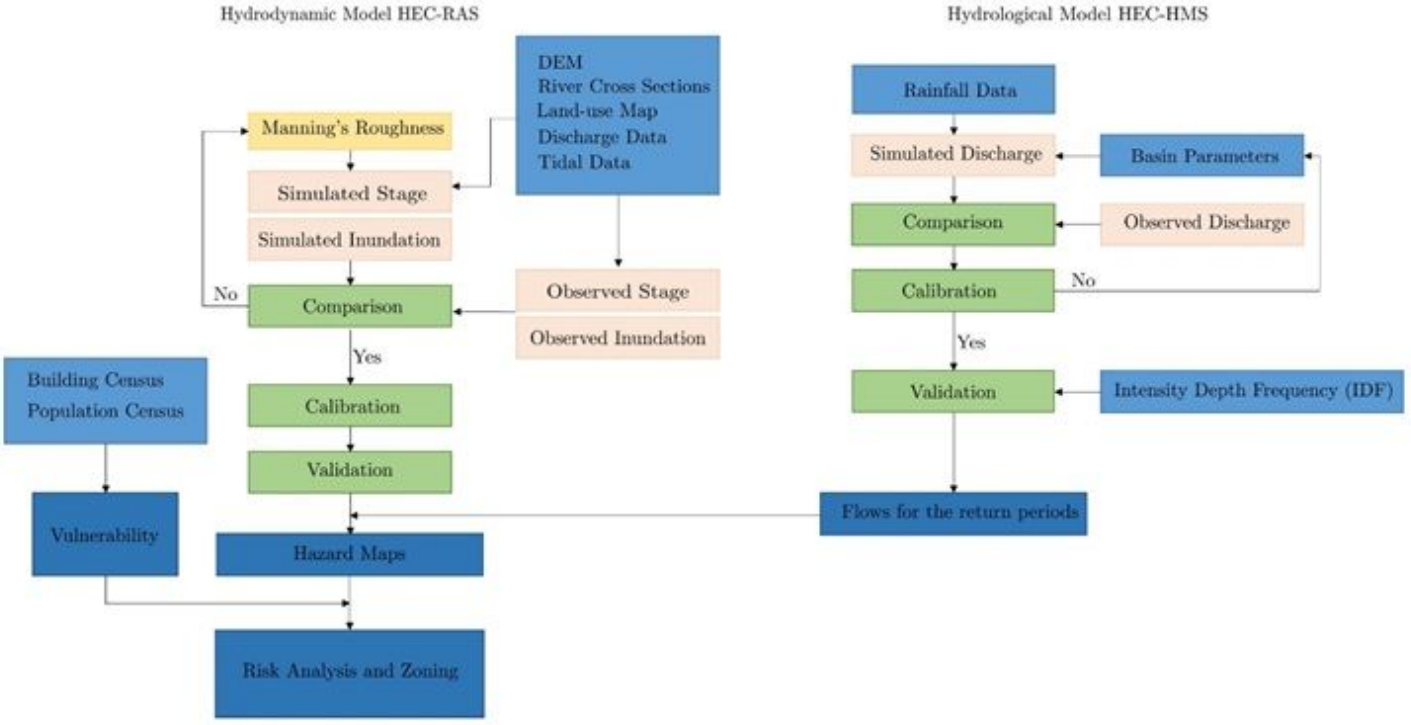

Figure 2

Illustration of the present modelling process.

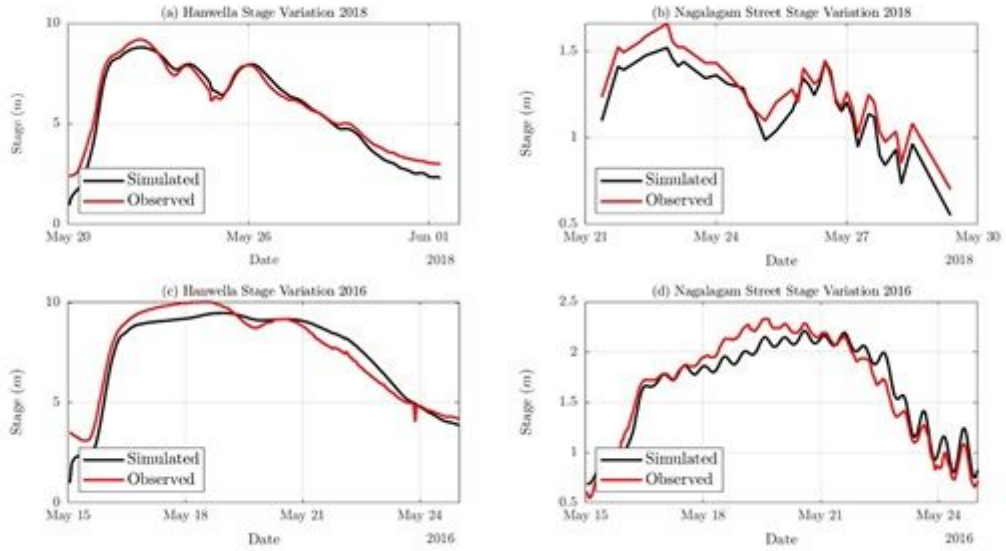

Figure 3

Comparison between simulated water level (black) and observed water level (red) for (a) May-2018 Hanwella Gauge (b) May-2018 Nagalagam Street Gauge (c) May-2016 Hanwella Gauge (d) May-2016

Nagalagam Street Gauge.

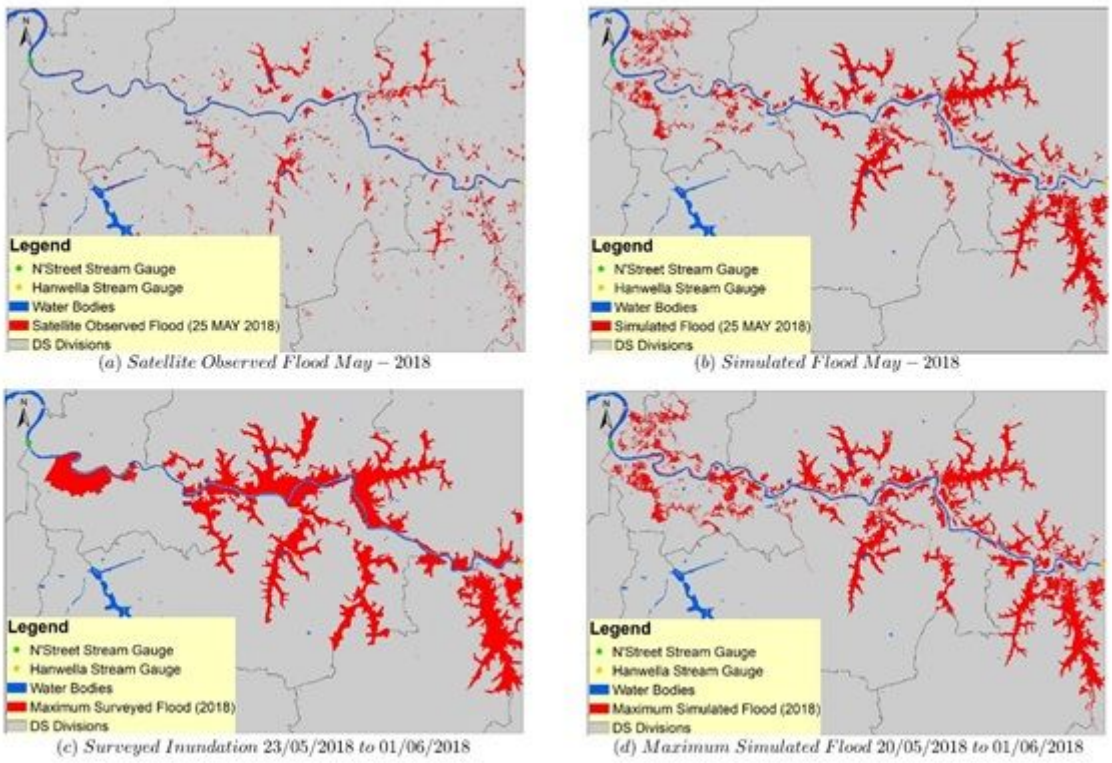

(a) *Satellite Observed Flood May – 2018*

(b) *Simulated Flood May – 2018*

(c) *Surveyed Inundation* 23/05/2018 *to* 01/06/2018

(d) *Maximum Simulated Flood* 20/05/2018 *to* 01/06/2018

Figure 4

(a) Observed flood extent extracted from Sentinel – 1 related to 25th May 2018 (b) Simulated flood 25th May 2018 (c) Surveyed inundation extent 23rd May 2018 to 01st May 2018 (d) Maximum simulated flood 20th May 2018 to 01st May 2018

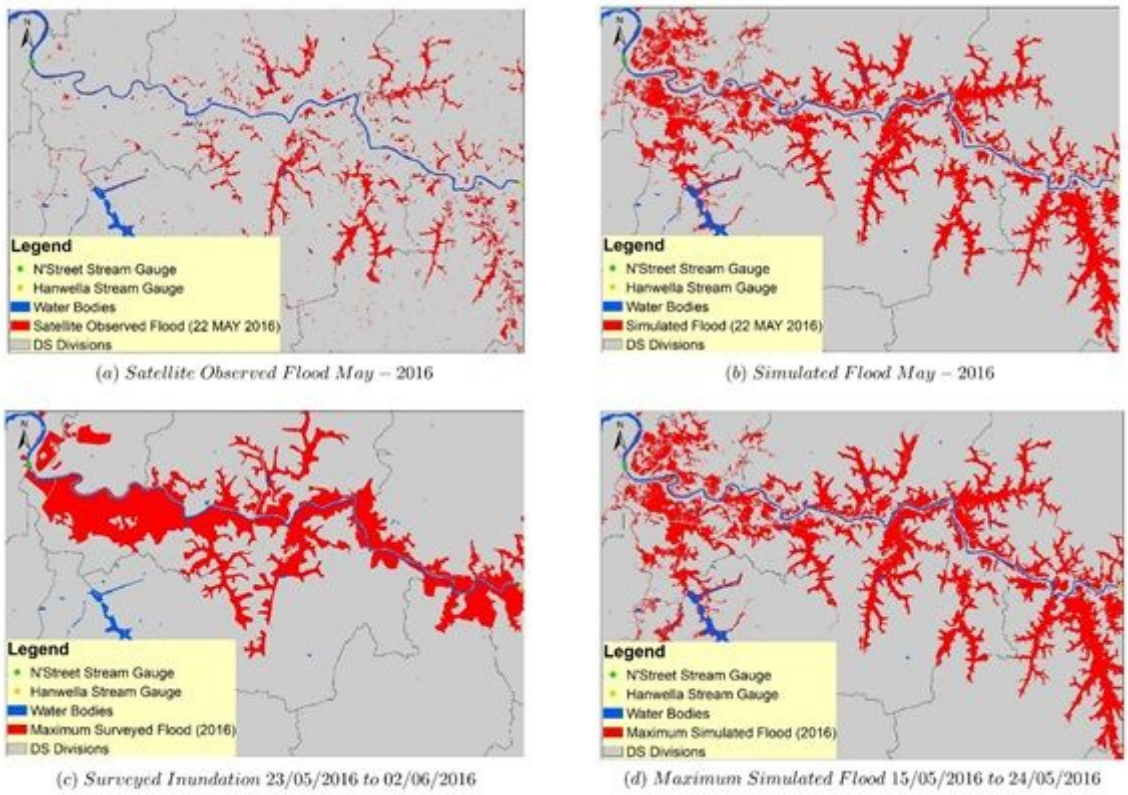

(a) *Satellite Observed Flood May – 2016*

(b) *Simulated Flood May – 2016*

(c) *Surveyed Inundation* 23/05/2016 *to* 02/06/2016

(d) *Maximum Simulated Flood* 15/05/2016 *to* 24/05/2016

Figure 5

(a) Observed flood extent extracted from Sentinel –1 related to 22nd May 2016 (b) Simulated flood 22nd May 2016 (c) Surveyed inundation extent 23rd May 2016 to 02nd May 2016 (d) Maximum simulated flood 15th May 2016 to 24th May 2016.

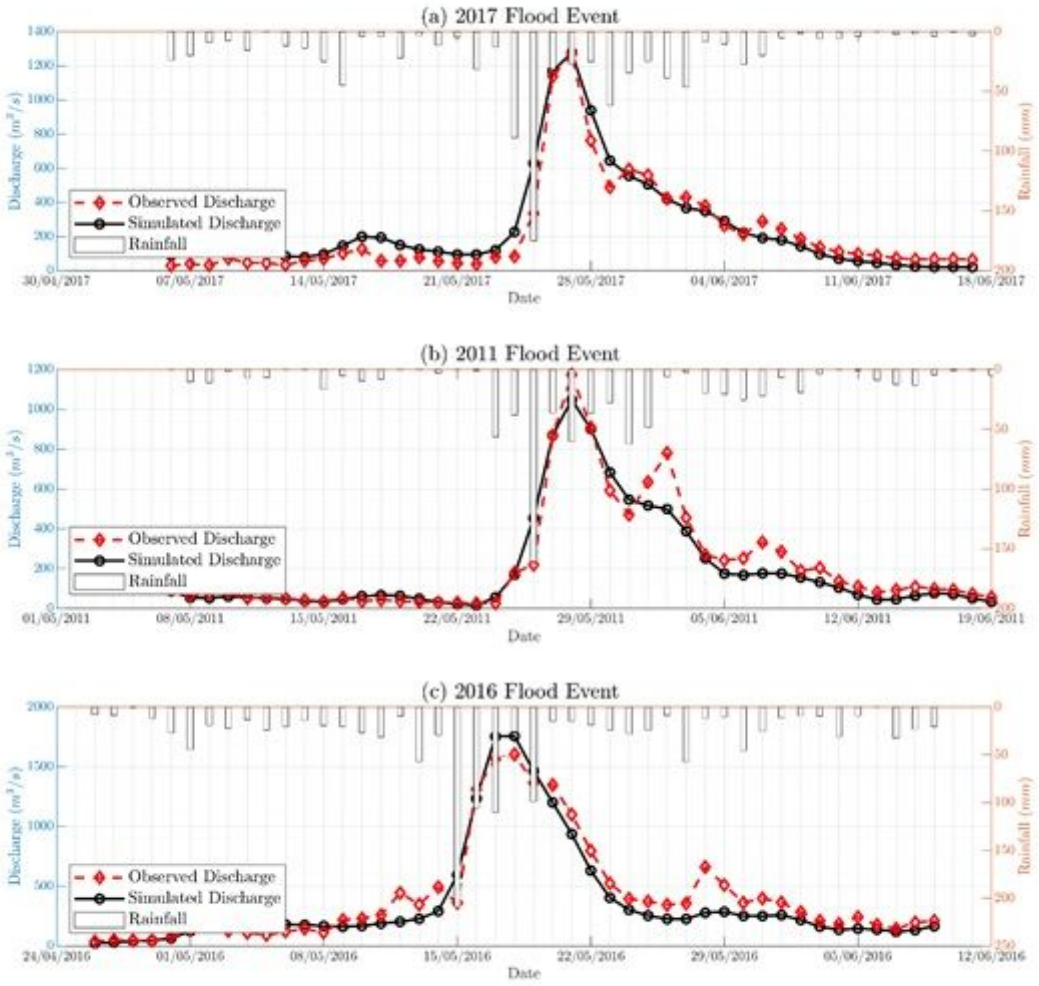

Figure 6

Comparison of discharge simulated with HEC-HMS model (black line with circles) and observed discharge (red dashed line with diamonds) in (a) 2017 Calibration, (b) 2011 Validation and (c) 2016 Validation flood events.

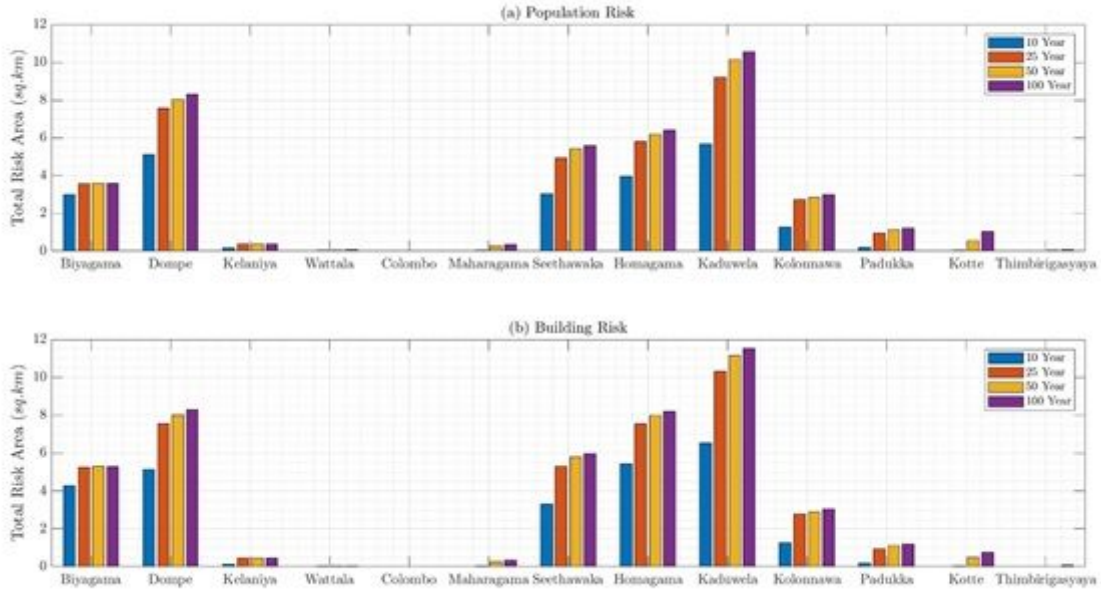

Figure 7

Total risk variation in terms of area under the different magnitude of floods (a) Population Risk (b) Building risk.

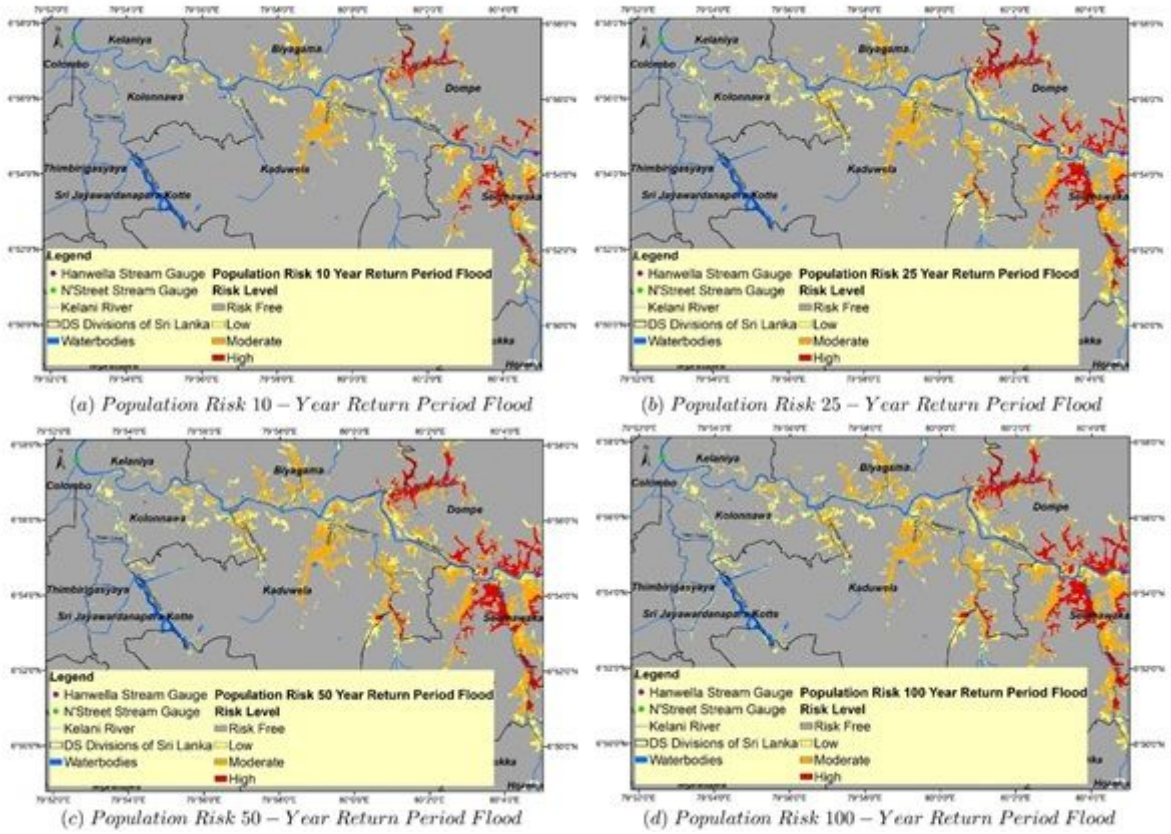

(a) Population Risk 10 – Year Return Period Flood

(b) Population Risk 25 – Year Return Period Flood

(c) Population Risk 50 – Year Return Period Flood

(d) Population Risk 100 – Year Return Period Flood

Figure 8

Population Risk Distribution (a) Population Risk under 10-year return period flood, (b) Population Risk under 25-year return period flood, (c) Population Risk under 50-year return period flood, (d) Population Risk under 100-year return period flood.

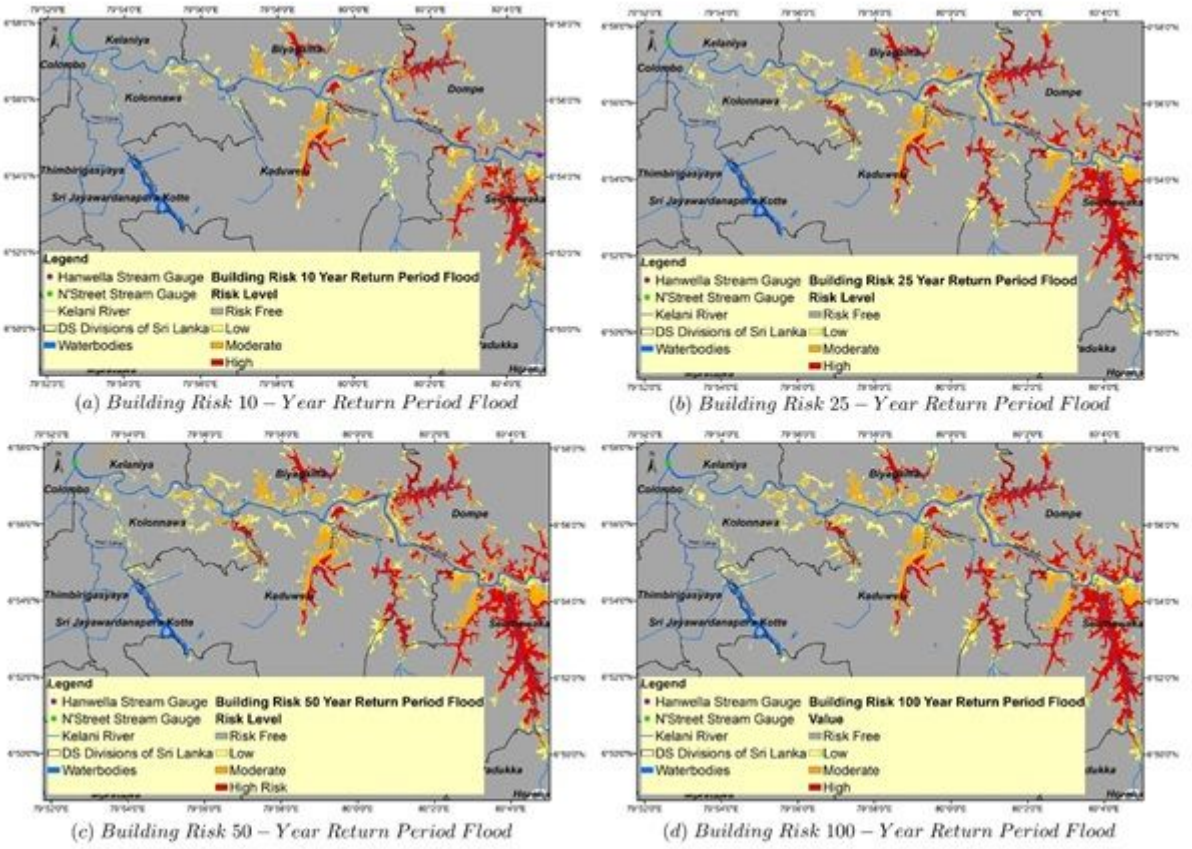

(a) Building Risk 10 – Year Return Period Flood

(b) Building Risk 25 – Year Return Period Flood

(c) Building Risk 50 – Year Return Period Flood

(d) Building Risk 100 – Year Return Period Flood

Figure 9

Building Risk Distribution (a) Building Risk under 10-year return period flood, (b) Building Risk under 25 - year return period flood, (c) Building Risk under 50-year return period flood, (d) Building Risk under 100-year return period flood.

Supplementary Files

This is a list of supplementary files associated with this preprint. Click to download.

- Supplementarytable.docx